Innovative Food Science and Emerging Technologies 74 (2021) 102838

Contents lists available at ScienceDirect

Innovative Food Science and Emerging Technologies

journal homepage: www.elsevier.com/locate/ifset

Component release after exposure of *Staphylococcus aureus* cells to pulsed electric fields

Víctor Freire [a], Giuseppe Lattanzio [b], Irene Orera [b], Pilar Mañas [a], Guillermo Cebrián [a,*]

[a] Departamento de Producción Animal y Ciencia de los Alimentos, Facultad de Veterinaria, Instituto Agroalimentario de Aragón - IA2 - (Universidad de Zaragoza-CITA), Zaragoza, Spain

[b] Proteomics Unit, Centro Investigaciones Biomédicas Aragón (CIBA), Instituto Aragonés de Ciencias de la Salud (IACS), Zaragoza, Spain

ARTICLE INFO

Keywords:
Food preservation
Non-thermal technologies
Microbial inactivation
Electroporation
Pore size

ABSTRACT

The objective of this work was to get further insights on the mechanism of inactivation of bacterial cells by pulsed electric fields (PEF) through the study of the release of intracellular components after exposing *Staphylococcus aureus* cells in McIvlaine buffer (pH 7.0, 2 mS/cm) to PEF treatments of different intensity (18 and 25 kV/cm) and treatment times (from 20 to 400 μs). Release of most compounds, except proteins, was almost immediate after the treatment, but the relative amount released depended on the molecule studied. A good correlation between the release of the smallest components studied (particularly ions) and membrane permeabilization (as measured by NaCl sensitization and PI entry) was observed. On the other hand, results obtained suggested that *S. aureus* inactivation by PEF would be related to the exit of cytoplasmic proteins of a molecular weight higher than 6 kDa. Results obtained in this work indicated that increasing PEF treatment time would reduce the capability of *S. aureus* cells to repair the electropores formed and suggested that this might be due to the formation of pores of a larger size, which *S. aureus* cells would be unable to reseal in a situation of homeostasis loss. *Industrial relevance:* Results reported here can help to design more effective treatments for microbial inactivation using PEF on food, and therefore facilitate its industrial implementation.

1. Introduction

Pulsed electric fields (PEF) is a non-thermal technology consisting in the application of very short high electric field (5–50 kV/cm) pulses to a food between two electrodes. This technology is considered an interesting alternative to current food preservation methods because it is capable of inactivating vegetative microorganisms (Álvarez, Condón, & Raso, 2006) while maintaining the organoleptic and nutritional properties roughly unchanged (Raso & Barbosa-Cánovas, 2003). In addition, since PEF is capable of enhancing mass-transfer processes, many other practical applications of this technology in the food industry, such as for extracting substances of interest or accelerating the drying rate in vegetables, have been investigated (Puértolas, Luengo, Álvarez, & Raso, 2012).

It is generally acknowledged that the bacterial envelopes would constitute the primary target of this technology (Mañas & Pagán, 2005). Thus, application of PEF would cause temporary or permanent permeabilization of cell membranes, a complex phenomenon called "electropermeabilization" or "electroporation" which has been widely investigated (Barbosa-Cánovas, Góngora-Nieto, Pothakamury, & Swanson, 1999; Ho & Mittal, 1996; Kinosita et al., 1991; Pavlin, Leben, & Miklavčič, 2007; Tsong, 1991; Weaver & Chizmadzhev, 1996). Among the several theories aiming to explain electroporation, the Zimmerman theory (Zimmermann, Pilwat, & Riemann, 1974), which proposes that the formation of pores is due to mechanical electrocompression, is the most accepted one. However, most of the available data about this phenomenon are based in experiments carried out with artificial membranes (Pavlin, Kotnik, Miklavčič, Kramar, & Maček Lebar, 2008), and eukaryotic cells (El Zakhem, Lanoisellé, Lebovka, Nonus, & Vorobiev, 2006) or from molecular dynamic (MD) simulations (Sözer, Levine, & Vernier, 2017; Tarek, 2005), being the amount of information obtained with bacterial cells very scarce.

As pointed out before, application of PEF can cause reversible (temporary) or irreversible (permanent) permeabilization of cell membranes. This is a phenomenon that has been observed in eukaryotes and in prokaryotes, and that depends on various factors (García, Gómez, Mañas, Raso, & Pagán, 2007). Irreversibly permeabilized bacterial cells would inevitably die. On the contrary, reversely permeabilized cells

* Corresponding author.
E-mail address: guiceb@unizar.es (G. Cebrián).

https://doi.org/10.1016/j.ifset.2021.102838
Received 8 April 2021; Received in revised form 15 September 2021; Accepted 20 September 2021
Available online 24 September 2021

might be able to reseal their envelopes and outgrow, given the appropriate recovery conditions are provided (García, Mañas, Gómez, Raso, & Pagán, 2006). Therefore, understanding the mechanisms and factors determining how and when reversible and irreversible permeabilization occurs is of the highest relevance since ultimately, this knowledge could lead to a better and rational design of PEF treatments in the future. This would definitely help the implementation in the industry of this technology.

On the other hand, given the difficulty of directly studying the occurrence and nature of membrane pores, the usual approach to study the electroporation phenomenon is to use indirect evidences, such as the measurement of the entrance (into the cell) of exogenous probes/molecules and/or the exit (from the cell) of certain biomolecules after PEF treatment (Aronsson, Rönner, & Borch, 2005; Batista Napotnik & Miklavčič, 2018; Saulis, Šatkauskas, & Pranevičiūtė, 2007). Unfortunately, studies designed to associate this entrance and/or exit of compounds with the biological processes involved in cell survival, such as the membrane repair process, are remarkably scarce. In addition, their observations cannot be applied to prokaryotes due to obvious differences in size, shape, metabolism, sublethal damage repair mechanisms and PEF treatment parameters used -higher electric fields and shorter pulse length treatments than for eukaryotes (Kandušer, Miklavčič, & Pavlin, 2009).

The objective of this work was to advance in the comprehension of PEF's inactivation mechanism in bacterial cells through the study of the release (amount and kinetics of exit) of intracellular components (such as ions, RNA and peptides and proteins) after exposure to PEF treatments of different intensity, in an attempt to correlate the phenomena of component exit with membrane permeabilization and resealing and, therefore, with microbial inactivation and sublethal injury repair. For this purpose, *Staphylococcus aureus,* a well know foodborne pathogen, was used as a model microorganism.

2. Materials and methods

2.1. Strains and growth conditions

The strain used in this study was *S. aureus* CECT 4459. For some experiments *S. aureus* RN4220 transformed with the pCN68 plasmid in order to constitutively express the Green Fluorescent Protein (GFP) (Wladyka et al., 2015) was also used. Bacterial cultures were maintained frozen at −80 °C in cryovials. Pre-cultures were prepared by inoculating 10 mL of tryptone soya broth (TSB; Biolife, Milan, Italy) supplemented with 0.6% (*w/v*) yeast extract (Biolife) (TSBYE) with a loopful of growth from a tryptone soy agar supplemented with 0.6% (w/v) yeast extract (Biolife) (TSAYE) plate. This pre-culture was incubated at 37 °C for 6 h, in a shaking incubator. Then, 50 μL of this pre-culture was inoculated into 50 mL of TSBYE and incubated at 37 °C for 24 h until cultures reached stationary-phase. For the RN4220 modified with the pCN68 plasmid, erythromycin (Sigma Aldrich, Steinheim, Germany) at a concentration of 10 μg/mL was added to the agar plate and the pre-culture.

2.1.1. PEF treatments

PEF treatments were performed using an exponential waveform pulse equipment previously described (Cebrián, Mañas, & Condón, 2015). High electric field pulses (Fig. 1) were produced by discharging a set of 10 capacitors via a thyristor switch (Behlke, HTS 160-500SCR, Kronberg, Germany) in a batch parallel-electrode treatment chamber. The capacitors were charged using a high voltage DC power supply (FUG, HCK 2500M 35000 Rosenhein, Germany), and a function generator (Tektronix, AGF 320, Wilsonville, OR, USA) delivered the signal to the switch. The gap between electrodes was 0.25 cm and the electrode area was 2.01 cm^2. Pulses (pulse width ≈ 4 μs) were applied at a frequency of 0.5 Hz to minimize sample heating. The actual electric field strength and electrical intensity applied were measured in the treatment chamber with a high voltage probe and a current probe, respectively, connected to an oscilloscope (Tektronix). The energy associated with pulses at electric field strengths of 18 and 25 kV/cm was 2.59 and 5.00, kJ/kg, respectively.

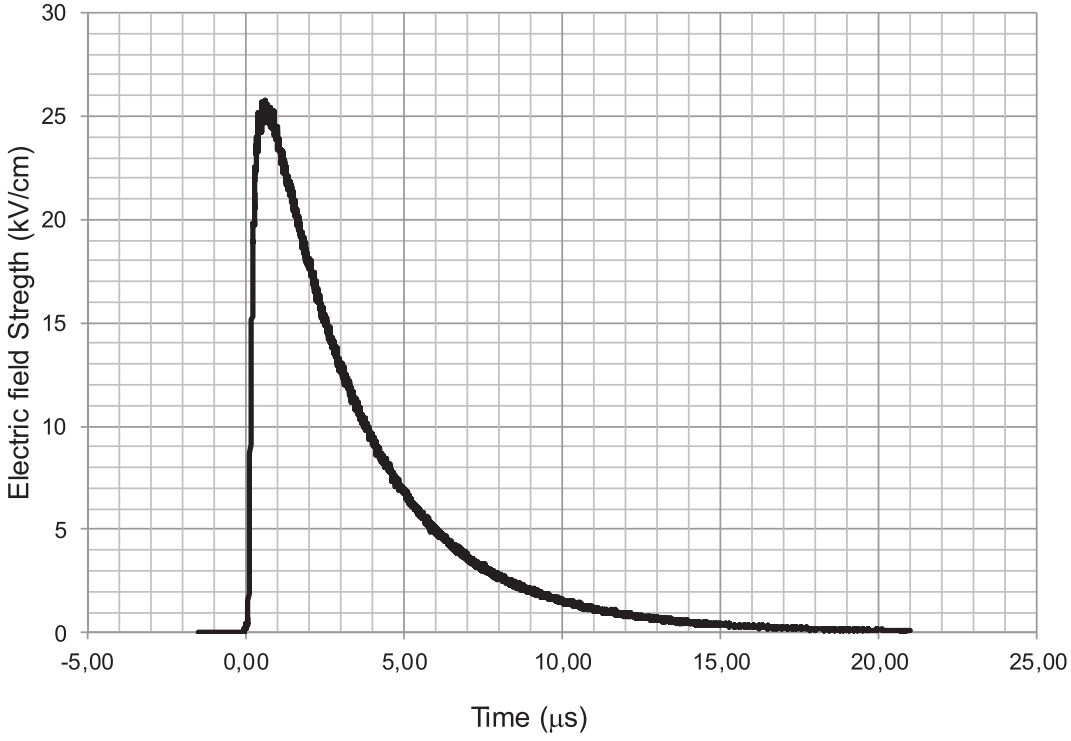

Fig. 1. Typical pulse used in this investigation.

Prior to PEF treatments, cells were centrifuged and resuspended in treatment medium, pH 7.0 McIlvaine buffer (Dawson, Elliot, Elliot, & Jones, 1974) which conductivity was adjusted to 2 mS/cm with distilled water using a conductivity probe (Alhborn, Almemo, Germany). The microbial concentration varied depending on the type of assay. Thus, for inactivation and permeabilization studies, a concentration of approximately 10^8 microorganisms/mL was used. For component release studies the microbial concentration was increased to approximately 10^{10} microorganisms/mL for methodological reasons (increasing analytical signal). In order to make meaningful comparisons, it was checked that microbial concentration in the range studied did not affect microbial permeabilization/resealing or inactivation/sublethal injury repair. The microbial suspension was placed into the treatment chamber with a sterile syringe and treatments were carried out at room temperature. Under the assayed conditions, the final temperature of the treatment media, measured as described by Raso, Alvarez, Condón, & Sala Trepat, 2000, was always below 35 °C. However, in order to check that the results obtained were not influenced by this increase in treatment temperature, for some experiments a tempered batch treatment chamber was used (Saldaña et al., 2010).

2.2. Recovery of PEF treated cells in solid media (TSAYE and TSAYE + NaCl)

The recovery medium used was TSAYE with or without the maximum non-inhibitory concentration (MNIC) of NaCl added (2.39 M) as described previously (Cebrián et al., 2015). After adequately diluting in 0.1% peptone water (Biolife), 0.1 mL samples were pour-plated and incubated for 24 h at 37 °C, unless NaCl was added. In this case, incubation was extended to 3–4 days. After incubation, colony forming units (CFU) were counted.

2.3. Recovery of PEF treated cells in liquid media (TSBYE and TSBYE + NaCl)

In order to determine the rate of recovery of tolerance to NaCl (sublethal injury repair), after PEF treatments, cells were diluted (1/10) in TSBYE or TSBYE +2.39 M NaCl and incubated at room temperature. Samples were collected at preset times and plated onto TSAYE and TSAYE +2.39 M NaCl.

2.4. Assessment of the percentage of cells with permeabilized membranes by PI staining

The fluorescent dye propidium iodide (PI; Sigma-Aldrich, 287,075) was used to evaluate cell membrane permeabilization by PEF treatments. PI is a fluorescent probe that is commonly used as a marker for membrane permeabilization since unaltered cell membranes prevent its entry inside the cell, where it bounds to nucleic acids leading to a 30-fold increase in its fluorescence (Arndt-Jovin & Jovin, 1989).

A stock solution of 1 mg PI in 1 mL of water was prepared. Samples of cell suspensions were centrifuged (14,500 rpm for 90 s), resuspended in McIlvaine citrate-phosphate buffer of pH 7.0 and mixed with PI solution to a final concentration of 1.5 μM before PEF treatments. After the treatments, cells were incubated for 10 min at room temperature avoiding light exposure. Previous experiments showed that the presence of PI in the treatment medium did not modify treatment conditions or microbial PEF resistance (data not shown).

The percentage of permeabilized cells was determined by microscopic examination using a Nikon Eclipse E4000 microscope (Nippon Kogaku KK, Japan) equipped with phase-contrast optics and an epifluorescence unit. In all cases, a × 40 objective was used, giving a total magnification of ×400. Cell counts were performed using at least two microscopic fields with high cellular concentration (more than 100 cells). The percentage of permeabilized cells was calculated by comparing the total number of cells, determined by using phase-contrast optics, with the number of cells showing fluorescence. Data were normalized by subtracting the percentage of untreated cells showing fluorescence, which was always lower than 2%. These normalized data were plotted as percentages of PI stained cells after the different PEF treatments.

The capability of PEF treated cells to reseal their membranes (recover their impermeability to PI) was determined in parallel to the liquid media recovery experiments described above. For this purpose, at the same preset times, cells were centrifuged (14,500 rpm for 90 s), resuspended in the same volume of pH 7.0 McIlvaine buffer and the percentage of permeabilized cells to PI was evaluated as described above.

2.5. Quantification and characterization of intracellular compounds released upon PEF treatments

In this work the release to the extracellular medium of several intracellular compounds was studied: ions (potassium and magnesium), RNA and peptides and proteins. *S. aureus* cells were PEF treated as previously described. In order to avoid interferences of the components of the growing media, cells were washed twice in pH 7.0 McIlvaine buffer before the treatments. Once treated, samples were centrifuged at 12000 ×*g* for 90 s and the pellet was discarded. The supernatant was filtered through a 0.22 μm filter (VWR, 28145–475, Radnor, Pensilvania, USA), and was either analyzed immediately or kept for further analysis at −80 °C in case of RNA samples, and − 20 °C for the rest of compounds. Protease inhibitor cocktail for bacteria (Sigma-Aldrich-P8465) was added to preserve those samples used for the electrophoretic study of the released proteins (see below). It was checked that preservation of samples under the indicated conditions did not resulted in RNA or protein degradation as compared to the samples immediately measured after the PEF treatment (data not shown).

In all the cases studied, besides the concentration of each released compound, its total soluble intracellular content (of the whole suspension) was also determined, in order to be able to determine the proportion of each compound released after PEF treatments. For that purpose, untreated cells were lysed with glass beads using a Beadbeater (BioSpec Products 3110BX Mini-BeadBeater, Bartlesville, Oklahoma, USA.) alternating 7 cooling (90 s) and lysis (30 s) cycles. Afterwards, the suspension was centrifuged at 14500 rpm for 90 s, filtered (0.22 μm filter, VWR) and the concentration of each of the compounds in the supernatant was determined as described below. The same lysis protocol was used for RNA and peptides and proteins determinations but not for ions. In the particular case of ions determinations, cell suspensions were subjected to a complete digestion with HNO_3, in such a way that the concentrations determined for ions correspond to the total cellular content (intracellular plus envelopes content).

The kinetics of release of each of the cellular compounds was also studied. For this purpose, PEF treated suspensions were incubated for different times (0–30 min) at room temperature and then processed as described above.

2.5.1. Quantification of K^+ and Mg^{2+} release from PEF treated cells

Supernatants and/or cellular suspensions obtained as described above were digested with HNO_3 (final concentration of 2% *v*/v) (Panreac, Barcelona, Spain) for 24 h, and the amount of K^+ and Mg^{2+} released was measured with an ICP (inductively coupled plasma) mass spectrometer (ELAN 6000, Perkin-Elmer, Germany) (Laborda, Medrano, & Castillo, 2004). Quantification was performed by specific calibration with K^+ and Mg^{2+} standards injected through the chromatographic system, in the same way that samples were measured. The percentage of K^+ and Mg^{2+} release was determined as the ratio between the amount of ions released (supernatant) and the total content present in untreated cells.

2.5.2. Quantification of RNA release from PEF treated cells

A broad range (20–1000 ng/μL) RNA quantification kit (Life Technologies, Q10210 Carlsbad, California, USA) was used to specifically measure the RNA with no interference of DNA, free nucleotides or proteins. In order to do so, manufacturer instructions were followed and Qubit 2.0 Fluorometer (Life Technologies, Q32866) was used. The percentage of RNA released was determined as the ratio between the amount of RNA released (supernatant) and the total soluble intracytoplasmic content (see above).

2.5.3. Quantification of protein release from PEF treated cells

Two protein quantification methods were tested: the Quick Start Bradford Reagent (BIO-RAD, 4110065A, Hercules, California, USA) and BCA techniques (Thermo Fisher, 23,225, Waltham, Massachusetts, USA) according to the microplate assay protocol described in the technical bulletins. Working conditions (dilutions, incubation time) were previously set up using Bovine Serum Albumin (BSA; Thermo Fisher, 23,225) as protein standard at concentrations between 0.01 and 2.00 mg/mL. Samples were incubated at room temperature for 5 min in the Bradford assay and at 37 °C for 30 min for BCA determinations. The absorbance was measured at 595 nm in the Bradford and 535 nm for BCA assays using a spectrofluorometer (Tecan GENios, Tecan, Mannerdorf, Suiza). The percentage of protein released was determined as the ratio between the amount of proteins released (supernatant) and the total soluble intracytoplasmic content (see above).

2.5.3.1. Electrophoretic study of the released proteins. After recovering the supernatants as previously described, samples were concentrated 10 times using a vacuum centrifuge (MEDEvac, miVac, DNA-23050-B00, England). Subsequently, concentrated samples were mixed in 1:1 proportion with a fresh solution of 2% β-mercaptoethanol (Merck, Darmstadt, Alemania) in Tricine Sample Buffer for Protein Gels (BIO-RAD) prior to their denaturalization (5 min at 100 °C). The molecular weight marker used was "Polypeptide SDS PAGE" (BIO-RAD) which contains 4.5 μg/μL of each of six proteins, ranging from 1.4 to 26 kDa. It was also mixed with sample buffer and denaturalized following manufacturer instructions.

Denaturalized samples and markers were run in pre-cast Tris-tricine gels containing 16.5% acrylamide (BIO-RAD, 4563064), at fixed potential of 100 V using a power supply (BIO-RAD, Power-Pack basic). After electrophoresis, proteins were fixed in the gels using a 40% methanol-10% acetic acid solution for 30 min, stained with a 0.025% Coomasie blue (Merck) and 10% acetic acid (Merck) solution for 1 h and then destained with a 10% acetic acid (Merck) solution in three consecutive steps of 15 min each. Later on, gels were stored in fixing solution at 4 °C and photographed using an image-analysis equipment (Syngene, Cambridge, United Kingdom). Protein content for each band was estimated with GeneTools v.3.08.03 (Syngene) software.

2.5.3.2. Protein identification

2.5.3.2.1. Protein digestion from gel. Protein bands were manually excised with scalpel, and in-gel digested with an automatic digestor (Intavis, Bioanalytical Instruments, Cologne, Germany). Briefly, bands were washed with water, ammonium bicarbonate (100 mM), and acetonitrile (ACN). Next, samples were reduced by incubation with DTT (10 mM) at 60 °C for 45 min and alkylated by incubation with iodoacetamide (50 mM) at room temperature for 30 min. Finally, proteins were digested overnight with trypsin at 37 °C (5 ng/μL, Trypsin Gold, Promega, WI, USA). Digestion was stopped by adding 0.5% TFA (trifluoroacetic acid), and tryptic peptides were extracted sequentially with increasing concentrations of acetonitrile in water.

2.5.3.2.2. Protein identification by LC-ESI-MS/MS. Protein identification was performed on a nano-LC system (LC425, Eksigent, Dublin, CA, USA) coupled to a hybrid triple quadrupole/linear ion trap mass spectrometer (4000 QTRAP, Sciex). After precolumn desalting, tryptic digests were separated on a C18 column (Acclaim PepMap100, 75 μm id, 15 cm, 3 μm particle size, Thermo Scientific, USA) at a flow rate of 300 nL/min, with a 30 min linear gradient from 5 to 30% of ACN in 0.1% formic acid. The mass spectrometer was interfaced with a nanospray source equipped with uncoated fused silica emitter tip (20 μm inner diameter, 10 μm tip, NewObjective, Woburn, MA) and was operated in the positive ion mode. MS source parameters were as follows: capillary voltage 2800 V, source temperature 150 °C, declustering potential (DP) 110 V, curtain and ion source gas (nitrogen) 20 psi, and collision gas (nitrogen) high. Analyses were performed using an information dependent acquisition (IDA) method with the following steps: single enhanced mass spectra (EMS, 400–1500 *m/z*) from which the six most intense peaks were subjected to an enhanced product ion [EPI (MS/MS)] scan. Protein identification was carried out using the Mascot search engine (Matrix Science Ltd.; versión 2.3) and the nonredundant databases SwissProt/UniprotKB (Release 2018_03; 557,012 sequences; 199,714,119 residues). Search parameters used were: missed cleavage 2, fixed modifications carbamidomethyl (Cys), variable modification oxidation (Met) and peptide and fragment mass tolerance 0.5 Da. Positive identification was assigned with Mascot scores above the threshold level (individual ions score > 44 and $p < 0.05$), at least two identified peptides with a score above homology, and similar experimental and theoretical molecular weight. We used the GO biological process annotation (http://www.geneontology.org) of the individual identified proteins and UniProt database information for manual classification into functional categories and identification of subcellular location.

2.5.3.3. Estimation of proteins' stokes radius. Estimated Stokes radius of the proteins was calculated using the Rippe & Stelin's, 1989 expression, which is assumed to be valid for globular proteins (Venturoli & Rippe, 2005). Molecular weights were calculated from the aminoacid (aa) sequences identified (see below).

2.6. Quantification of GFP release from S. aureus PEF treated cells

GFP release quantification was carried out with *S. aureus* strain RN4220 transformed with the pCN68 plasmid, using a spectrofluorometer (Tecan GENios). In order to do so, 200 μL of the supernatant (previously centrifuged and filtered as described above) from PEF treated cells, was placed in microtiter plates and fluorescence was measured with an excitation wavelength of 485 nm and emission wavelength of 510 nm.

2.7. Experimental replicates and statistical methods

All determinations were performed at least three times in independent working days and with different microbial cultures, except recovery in liquid media/resealing experiments that were performed in duplicate on independent working days (also with different cultures).

Statistical analysis (ANOVA, Student-t and Pearson's correlation tests) were performed using GraphPad PRISM (GraphPad Software, San Diego, CA). Error bars in figures correspond to the mean standard deviation.

3. Results

3.1. Impact of electric field strength and treatment time on S. aureus electroporation and survival after PEF treatments

Fig. 2 shows the survival curves of *S. aureus* cells to PEF treatments at two different electric field strengths (18 and 25 kV/cm). Cells were recovered in non-selective (TSAYE) and selective (TSAYE-NaCl) media. As described previously (Cebrián et al., 2015) recovery in non-selective media allows quantifying the amount of irreversibly damaged cells, while recovery in selective media allows quantifying the amount of

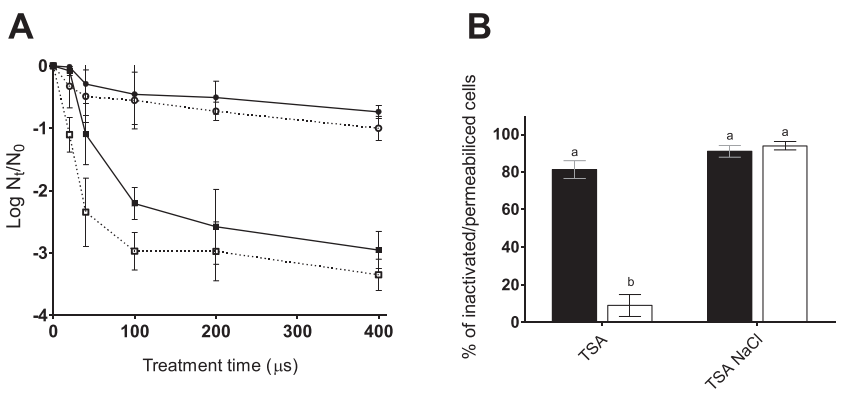

Fig. 2. A) Survival curves at 25 kV/cm (■, □) and 18 kV/cm (●, ○) of *S. aureus* cells recovered in TSAYE (full symbols ■, ●) or TSAYE-NaCl (empty symbols □, ○). B) Percentage of *S. aureus* cells inactivated (recovered in TSAYE) or permeabilized (recovered in TSAYE NaCl) after PEF treatments of 18 kV/cm – 400 μs (black bars) and 25 kV/cm – 20 μs (white bars). Error bars represent the standard deviations. Different letters indicate statistical significant differences ($p < 0.05$) between treatment and/or recovery conditions (ANOVA).

electroporated (i.e. permeabilized) cells. Preliminary experiments also revealed that, under our experimental conditions, the number of electroporated cells as determined by plating in TSAYE+ 2.39 M NaCl was comparable to that determined by PI staining (data not shown) as previously reported (Cebrián et al., 2015). From all of the indicated above, it can be deduced that the difference between the number of recovered cells in both media would correspond to the proportion of cells that, despite being permeabilized, could repair the damages suffered, remain viable and outgrow in non-selective media.

As can be observed in Fig. 2A, the number of electroporated and inactivated *S. aureus* cells was higher the higher the electric field strength and the longer the treatment time applied, as a general trend. On the other hand, it can also be observed that after PEF treatments at 18 kV/cm -and regardless of the duration- the difference between the number of permeabilized and inactivated cells was below 0.25 log cycles, i.e. almost all the permeabilized cells were inactivated. However, given the low level of inactivation attained and the low accuracy of plate count methods (Cebrián et al., 2015) this later conclusion should be taken with care. By contrast, after treatments of up to 100 μs at 25 kV/cm, a difference of approximately one log cycle was observed between the number of permeabilized and inactivated cells, indicating that these treatments led to the generation of a larger proportion of cells capable of repairing the damages caused by PEF. In any case, it should be noted that after treatments of more than 100 μs at 25 kV/cm no significant differences ($p > 0.05$) between the number of cells recovered in both media was observed, what means that increasing treatment time also led to a progressive decrease in the proportion of cells capable of repairing the damages caused by PEF at this higher electric field strength. Finally, it was observed that treatments at 25 kV/cm for 20 μs and at 18 kV/cm for 400 μs caused a similar degree of permeabilization (90%) but their lethality was remarkably different, approximately 10% and 90%, respectively (Fig. 2B).

3.2. Leakage of intracellular compounds

For all the molecules studied in this work the influence of post-treatment incubation time on the amount released after PEF treatments was studied as a first step (Fig. 3). The major objective of these experiments was to determine the post-treatment incubation time required for the complete release of intracellular compounds from electro-permabilized *S. aureus* cells (15 min). For this purpose, a fixed PEF treatment (18 kV/cm and 400 μs) was used. Then, the impact of the electric field strength and treatment time on compound leakage was assessed, using the previously determined post-treatment incubation time of 15 min (Fig. 3).

3.2.1. Ions

The amount of K^+ and Mg^{2+} ions released to the extracellular medium from *S. aureus* PEF treated cells (18 kV/cm; 400 μs) after different incubation times is shown in Fig. 3A. As it can be observed, the concentration of both ions in the extracellular media was similar regardless of the duration of the post-treatment incubation time. This would imply that exit of both ions was very fast, almost immediate, reaching the maximum leaked concentration in less than 1 min after PEF treatments. On the other hand, it can also be observed that the application of a higher electric field strength resulted in higher ion leakages from the cells (Fig. 4A), and that longer treatments times, up to 200 μs, also lead to an increase in the amount of ions released.

If the release of K^+ and Mg^{2+} ions is compared it can be observed that in all the cases the amount of K^+ released was higher than that of Mg^{2+}, either in absolute (amount released) or in relative terms (% of the total cellular content released). Thus, the more intense treatments provoked the loss of approx. 98% of the total cellular K^+ content, while in the case of Mg^{2+} the maximum release was lower than a 20% of the total cell content even after treatments of 25 kV/cm – 400 μs, which led to the permeabilization of approximately 99.9% of the cells' population (Fig. 2). The most probable explanation could be that K^+ ions are mostly free in the cytoplasm, while Mg^{2+} is usually found associated to proteins and/or nucleotides (Vinothkumar & Henderson, 2010).

3.2.2. RNA

RNA leakage, as described for ions, was an almost instantaneous phenomenon, as can be observed in Fig. 3B. Also like in the case of ions, RNA release increased as the treatment time and electric field strength increased until reaching a maximum of around 10% of the total RNA cellular content (Fig. 4B). Given the size of the proteins released (see below) it can be hypothesized that this would correspond to the exit the smallest RNAs, including the smallest mRNA, tRNA and miRNA (Gerstberger, Hafner, & Tuschl, 2014).

3.2.3. Peptides and proteins

As described in material and methods, the leakage of peptides and proteins was quantified through the BCA and Bradford techniques. Marked differences in the concentration of proteins released were found depending on the quantification method used. Thus, the amount of protein released from *S. aureus* cells after PEF treatments was much lower when determined using the Bradford technique (Figs. 3C and 4C). In this way it should be noted that, as stated in its technical bulletin, the Bradford method detects proteins with an estimated minimum size of 3–5 kDa (Chutipongtanate, Watcharatanyatip, Homvises, Jaturongkakul, & Thongboonkerd, 2012). Therefore, it is not adequate for quantifying peptides and low molecular weight proteins. Results obtained also indicate that the maximum concentration of protein released was reached after 15 min of incubation after the PEF treatment (Fig. 3C). On the other hand, and as can be observed in Fig. 4C, increasing the electric field strength or the treatment time led to an increase in the protein concentration released to the extracellular medium.

GFP release from *S. aureus* cells (using a *S. aureus* strain containing a

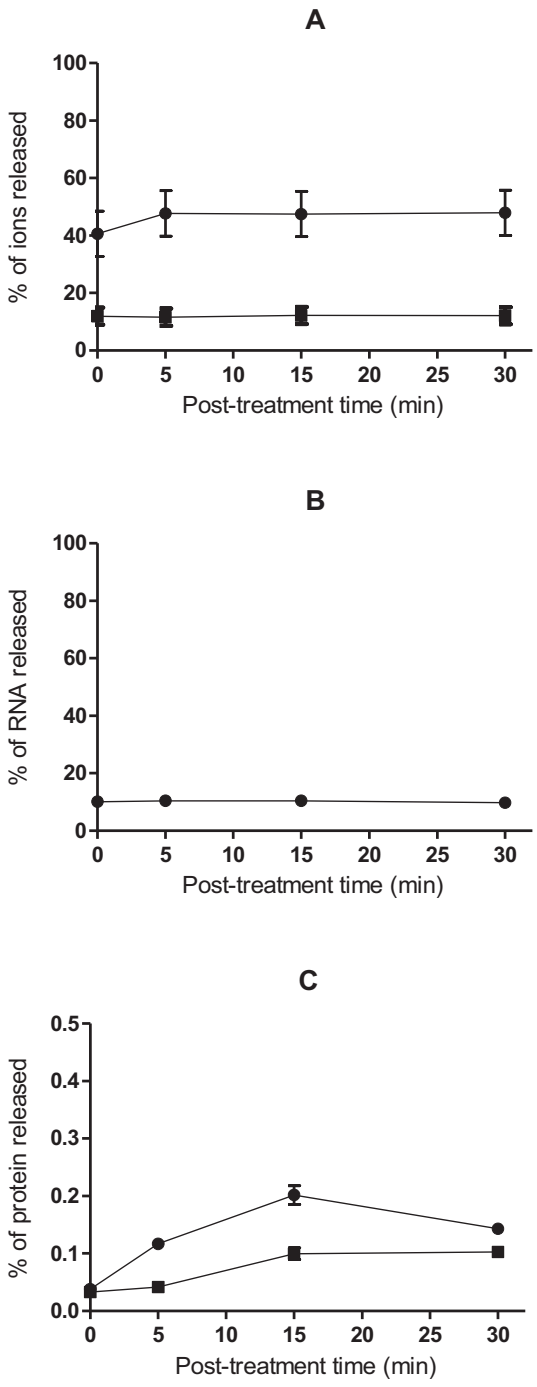

Fig. 3. Influence of post treatment time incubation in the percentage (of the total cellular content for ions and of the total intracytoplasmic soluble content for RNA and proteins) of A) K^+ (circles) and Mg^{2+} (squares), B) RNA, and C) protein measured by BCA (circles) and Bradford (squares), released from *S. aureus* PEF treated cells after 18 kV/cm – 400 μs PEF treatments. Error bars represent the standard deviations.

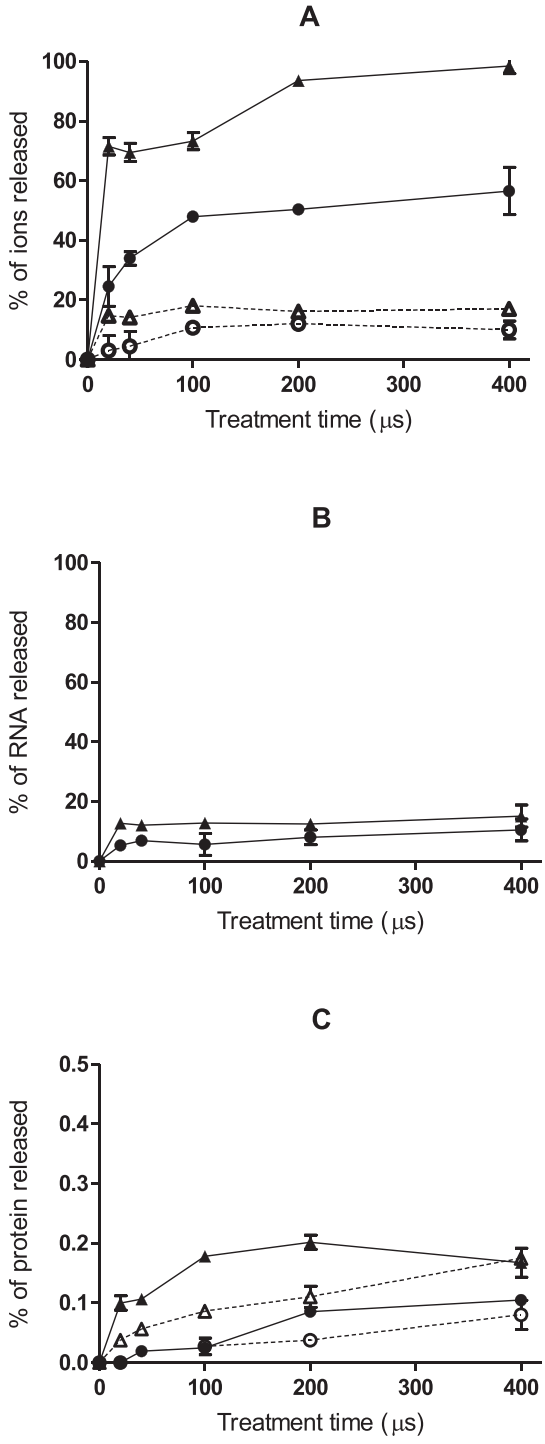

Fig. 4. Influence of treatment time and electrical field strength (18 kV/cm, circles; 25 kV/cm: triangles) on the percentage (of the total cellular content for ions and of the total intracytoplasmic soluble content for RNA and proteins) of A) K^+ (full symbols) and Mg^{2+} (empty symbols), B) RNA, and C) protein measured by BCA (full symbols) and Bradford (empty symbols and dashed lines) released from *S. aureus* PEF treated cells. Error bars represent the standard deviations.

plasmid coding for this protein) was also studied because this method might offer a higher sensibility for studying protein exit, as compared to Bradford and BCA. However, results obtained showed no quantifiable exit of GFP after *S. aureus* cells were PEF treated even under the most intense conditions (25 kV/cm – 400 μs).

3.3. Characterization of proteins leaked to the medium

3.3.1. Electrophoretic characterization of released proteins

Preliminary experiments (filtration using centrifuge filters with a cut off of 20 kDa and SDS-PAGE Tris-Glicine gels) evidenced that the

proteins released were of a size smaller than 20 KDa (data not shown). Therefore, the concentrated supernatants from *S. aureus* PEF treated cells were run on SDS-PAGE Tris-Tricine gels. As described above, the influence of post-treatment incubation time (kinetic of exit) was studied first and, then, the influence of the electrical field strength and treatment time on the amount and size of proteins released was studied. As a way of example, Fig. 5 shows the electrophoretic pattern of the supernantants of *S. aureus* PEF treated cells (18 kV/cm; 400 μs) after different post-treatment incubation times (0–30 min). Fig. 6 includes the concentration of released protein calculated through band intensity measurements from gels, as a function of post treatment time (6A) and electric field strength and treatment time (6B).

As can be observed in Fig. 5 two bands of around 8.5 and 6.7 kDa could be distinguished after PEF treatments. It should also be noted that the concentration of protein in each lane estimated by comparison with the marker was substantially lower than that estimated by BCA prior to gel running. This can be attributed to the presence of small peptides and amino acids which would not fixate properly and would diffuse during destaining steps as occurred with the sixth band of the ladder of approximately 1.4 kDa.

The intensity of the bands (protein concentration) increased with post-treatment incubation time, which suggests that protein exit would be more related to diffusion processes than to electrophoretic processes taking place during exposure to PEF (Figs. 5 and 6A). On the other hand, leakage of these protein fractions significantly increased with treatment time but, conversely to that observed for BCA and Bradford assays, did not increased with the electric field strength (Fig. 6B). Further work will be required in order to determine the causes of these differences.

3.3.2. Protein identification by LC-ESI-MS/MS

Table 1 includes the proteins identified (as described in materials and methods) from the two bands. It also includes their identity score and some of their more relevant characteristics: molecular weight, stokes radius calculated as described in materials and methods, and cellular localization and function. Two different proteins (Thioredoxin TrxA, and Phosphocarrier protein HPr) were identified in band 1 (≈8.5 kDa) and one protein (Copper Chaperone CopZ in band 2 (≈6.7 kDa). The size of TrxA, HPr and CopZ was consistent with their observed electrophoretic mobility. It should be remarked that all the identified proteins were cytoplasmic. This is of the highest relevance since it confirms that we were measuring the exit of cytoplasmic components, and not the release of components from the membrane and/or the cell wall.

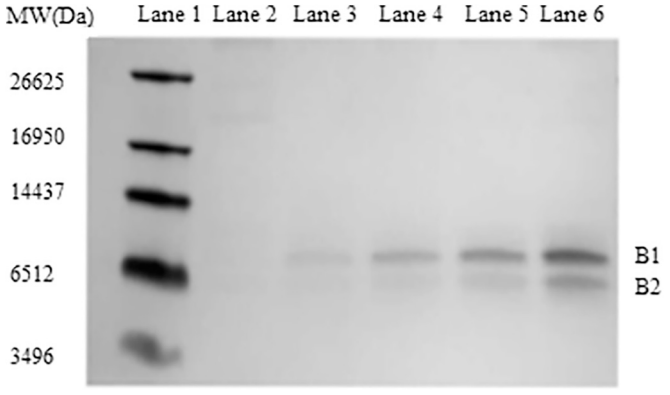

Fig. 5. Influence of post treatment time incubation on the electrophoretic profiles (Tris-Tricine 16.5% acrylamide gels) of proteins released after 18 kV/cm – 400 μs PEF treatments. Lane 1: molecular weight marker. Lane 2: Control (untreated cells). Lane 3: No incubation after PEF treatment. Lane 4: Suspensions incubated for 5 min. Lane 5: Suspensions incubated for 15 min. Lane 6: Suspensions incubated for 30 min. B1: Band 1 (≈8.5 kDa); B2: Band 2 (≈6.7 KDa).

3.4. Relationship between component exit and S. aureus electroporation/inactivation

The potential existence of a relationship between the exit of each of the components studied (% relative to the total cellular content) and the degree of electroporation and inactivation (in log cycles) of *S. aureus* cells after different PEF treatments (the two electric field strengths and six treatment times studied) was examined through the Pearson's correlation coefficient. Results obtained are included in Table 2, which also includes the estimated p values. A significant relationship ($p < 0.05$) between *S. aureus* electroporation and the exit of ions, RNA and proteins measured with BCA was determined. By contrast, *S. aureus* inactivation cells only showed a significant correlation ($p < 0.05$) with the percentage of Mg^{2+} released and the intensity of Bands 1 and 2 in electrophoretic gels. Similar results were obtained if these comparisons were established using the % of permeabilized and inactivated cells instead of the log cycles of inactivation (data not shown) Although these correlations should be taken with care given the low accuracy of the plate count methods, these results suggest that *S. aureus* inactivation by PEF might be related somehow to protein exit or, more precisely, to the exit of proteins of a molecular weight higher than 6 kDa, approx. Furthermore, if treatments leading to the same level of permeabilization but to different inactivation levels, such as 18 kV/cm - 400 μs and 25 kV/cm - 20 μs (Fig. 2B) are compared, it can be observed that the amount of ions, RNA and protein as measured by means of the BCA technique released was very similar for both treatments (Fig. 7A), but the amount of protein as measured by the Bradford technique and the intensity of the 8.5 and 6.7 kDa bands was significantly higher after the treatment leading to the higher inactivation level (18 kV/cm - 400 μs) (Fig. 7B and C).

3.5. Pore resealing and sublethal damage repair

Finally, in order to study the processes of pore resealing and membrane damage repair after PEF treatments, PEF treated *S. aureus* cells were recovered in parallel in two different liquid media, a non-selective (TSBYE) and a selective one (TSBYE-NaCl). Thus, after the PEF treatment and at preset time intervals, samples were taken from the two recovery media and the percentage of cells with membranes permeable to PI and that of sublethally damaged cells (estimated by selective plating as described in material and methods) was determined.

As it can be observed in Fig. 8A, *S. aureus* cells incubated in TSBYE after a PEF treatment of 25 kV/cm and 20 μs, progressively recovered membrane impermeability, both to PI and to NaCl. This observation concurs with previously published data indicating that, for eukaryotic cells, the resealing process (reduction of pore size) would also be gradual (Saulis, 2010). It can also be observed that recovery of impermeability to PI seemed to precede recovery of NaCl-impermeability. On the other hand, when these same cells were incubated in TSBYE-NaCl (Fig. 8B), *S. aureus* sublethally damaged cells could not recover viability and died progressively. Nevertheless, even under these conditions, a significant proportion of electroporated cells were able to recover their impermeability to PI even though this was not enough to recover viability, as previously observed (Cebrián et al., 2015).

Since, as demonstrated in Fig. 8B, PEF treated *S. aureus* cells were able to reseal their membrane in such unfavorable conditions, we reproduced this experiment using cells exposed to conditions (18 kV/cm - 400 μs) leading to a similar level of cell permeabilization (90%) but without the presence of sublethally damaged cells. In this case, and conversely to what it was observed for cells exposed to 25 kV/cm for 20 μs, *S. aureus* cells were not able to recover their impermeability to PI in none of the studied conditions (Fig. 8C and D).

4. Discussion

In this work, the release of cellular components from *S. aureus* cells after exposure to PEF treatments leading to different inactivation and

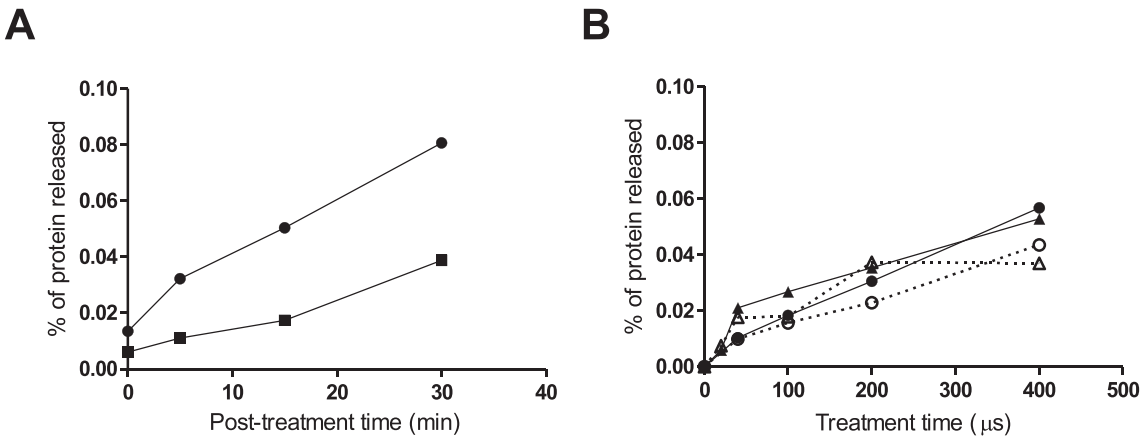

Fig. 6. A) Influence of post treatment time incubation on the percentage (of the total intracytoplasmic soluble content) of protein released (from *S. aureus* PEF treated cells quantified by measuring band intensity in Tris-Tricine gels after 18 kV/cm – 400 μs PEF treatments. Band 1 (circles) and Band 2 (squares). B) Influence of treatment time and electrical field strength (18 kV/cm: circles; 25 kV/cm: triangles) on the percentage of protein released (15 min of post treatment time) from *S. aureus* PEF treated cells quantified by measuring band intensity in Tris-Tricine gels. Band 1 (full symbols) and Band 2 (empty symbols and dashed lines). Figures show representative results. Band 1 and Band 2 correspond to the bands identified in the electrophoretic gels of Fig. 4.

permeabilization levels was studied. The amount and kinetic of leakage of several intracellular compounds (ions, RNA, and proteins, including GFP) was investigated and compared with the level of permeabilization to PI, NaCl sensitization, cell inactivation and pore resealing/membrane repair ability in order to get further insights into the mechanisms of bacterial inactivation by PEF.

The number of studies dealing with component exit after PEF treatments in prokaryotes is scarce. However, data obtained in this work are in agreement with previously published results, as increasing the severity of the PEF treatment (treatment time and/or electric field strength) lead to higher permeabilization and intracellular compounds exit, as it was described for K^+ release (Saldaña et al., 2010; Saulis, 2010), for ATP and UV absorbing intracellular compounds leakage in *E. coli* and *L. innocua* (Aronsson et al., 2005; Matos et al., 2013) and protein release in *E coli* (Meglic, Marolt, & Miklavcic, 2015; Oshima & Sato, 2004). It should also be noted that, as described by Aronsson et al. (2005), our results indicate that the relative amount of compounds released form *S. aureus* cells was higher for the smaller molecules such as ions, although in other studies releases up to 90% of the total cellular content of proteins and/or RNA molecules has been documented (Matos et al., 2013; Oshima & Sato, 2004). These differences might be mainly attributed to the different experimental conditions studied and methodology employed (Electric field, pulse length, different incubation times after the treatments etc.), but wide differences depending on the species studied have also been observed (Aronsson et al., 2005).

Results obtained also revealed that whereas smaller molecules (such as ions and even RNA) were released almost instantaneously, the larger molecules studied (proteins) displayed a more progressive exit. This behavior might be explained on the basis of the differences in size of the different molecules (see below) but also on other factors such as their different shape and charge (Saulis, 2010). It should also be noted that the concentration gradient for ions, e.g. *S. aureus* has a K^+ cytoplasmic concentration of 0.5–1.5 M even when the extracellular concentration is in the millimolar range (Christian & Waltho, 1964; Graham & Wilkinson, 1992), is much higher than that of any protein. In addition, our results also suggest that protein exit would probably mainly occur by means of diffusion, at least for low molecular weight proteins, and not due to electrophoresis.

According to data obtained in this work, application of PEF treatments consisting of microsecond pulses (approximately 4 μs) in the range between 18 and 25 kV and a total treatment time of 20–400 μs to *S. aureus* cells would lead to the generation of pores with a radius higher that 0.7 nm, which would allow the exit of K^+, Mg^{2+} and the uptake of PI (Azarashvili et al., 2011; Bowman, Nesin, Pakhomova, & Pakhomov, 2010; Hille, 1975; Vinothkumar & Henderson, 2010) but would not allow the exit of proteins with a stokes radius of 2.5 nm, thus preventing GFP (Mw = 26.8 KDa, (Matos et al., 2013)) release. In any case, our estimations should be taken just as rough approximation of the pore size, for various reasons. First, because determining the exact molecular radius of a molecule is difficult due to different phenomena such as the hydration degree of molecules (Hille, 2001); moreover, as it has been previously indicated, transmembrane transport is also conditioned by shape and charge (Saulis, 2010). Secondly, it should be reminded that *S. aureus* possess a very thick and dense cell wall whose "pores" could be as small as 2.3 nm, according to the model proposed by Kim, Chang, and Singh (2015), that might also affect transmembrane transport processes, as previously demonstrated for proteins (Chan, Frankel, Missiakas, & Schneewind, 2016). This would mean that the size of the pores formed might be higher and that GFP release would be limited by the low permeability of the staphylococcal cell wall and not by the size of the electropores formed. However, it should also be noted that GFP release was observed after exposing *S. aureus* cells to BacSp222, a peptide which is thought to specifically act on the bacterial membrane, what would indicate that GFP can indeed cross the *S. aureus* cell wall (Nowakowski et al., 2018; Wladyka et al., 2015). And, finally, because although no protein nor RNA degradation was observed along the frozen storage period -between sample collection and measurement- as has been indicated in materials and methods, it cannot be discarded that these phenomena might have taken place during the PEF treatment and the subsequent incubation period (15 min). Nevertheless, our results strongly suggest that, at least for proteins, this was not the case. Thus, the electrophoretic profiles of the *S. aureus* supernatants showed no smearing and only two well defined bands were consistently obtained in Tris-Tricine gels, regardless of the treatment length and the subsequent incubation time assayed. In addition, the theoretical molecular weight of the proteins identified via LC-ESI-MS/MS reasonably matched with that determined experimentally, indicating that, at least these proteins, were not degraded. In any case, the radius pore size values estimated in this work are much smaller than those reported by Gowrishankar, Esser, Vasilkoski, Smith, and Weaver (2006) and by Krassowska and Filev (2007) who estimated an average pore radius of 10 and 20 nm in their simulations of treatments at 0.40 kV/cm for 100 μs and 1 ms, respectively. These authors estimated that some pores would reach a radius above 400 nm. Conversely, Saulis and Saulė (2012) measured pores radius smaller than 0.8 nm in around 70% of Hepatoma MH-22A cells after treatments at 1.0 kV/cm for 100 μs. These differences might be attributed to the differences in cell's size, cell's peptidoglycan structure and thickness, field strength, pulse and treatment lengths and

Table 1
Protein species identified in 1D-SDS-PAGE gels.

Band	Protein	Species	Uniprot entry	Score/ pep/ion	Coverage %	Mw th	Mw exp	Stokes radius (nm)	Location	Function	GO (BP)	Sequences
1	Thioredoxin	*S. aureus*	Q2FZD2	112/5/2	24	11,790	8567	1.80	Cytoplasm	Cell redox homeostasis Glycerol ether metabolic process	GO:0045454 GO:0006662	K.ENLAEVLDK·H K.LDVDENPSTAAK·Y
1	Phosphocarrier protein HPr	*S. aureus*	P0A0E3	95/4/2	32	9496	8567	1.66	Cytoplasm	PEP-dependent sugar PTS Carbohydrate transport	GO:0009401 GO:0008643	K.FDSDIQLEYNGK·K K.SIMGVMSLGVGK·D + 1 or 2 Oxidation (M)
2	Copper chaperone	*S. aureus*	P0C885	52/2/2	28	7237	6717	1.49	Cytoplasm	Metal ion transport	GO:0030001	K.DAIEDQGYDVV.-K. VAVSQMKDAIEDQGYDVV.- + Oxidation (M)

Positive identification was retained with Mascot scores above the threshold level (individual ions score > 44 and $p < 0.05$), at least two identified peptides with a score (pep/ion) above homology and similar experimental and theoretical MW. We used the GO biological process annotation (http://www.geneontology.org) of the individual identified proteins and UniProt database information for manual classification into functional categories and identification of subcellular location.

experimental models used but also to the fact that, in our work, we have estimated the size of the molecules passing through the pores and not the pore radius itself.

Data obtained in this work also demonstrate that there is a good correlation between *S. aureus* membrane electroporation and the exit of low molecular weight compounds such as ions, and even with RNA and peptides. However, it seems that neither the generation of pores nor the exit of these low molecular weight compounds will directly cause *S. aureus* cell's death. Therefore, other phenomena should take place in order to make *S. aureus* electroporated cells unviable. A possible explanation for these results would be that pores need to grow until a particular size until electroporation becomes irreversible. In this way, the high correlation between the intensity of the bands in electrophoretic gels corresponding to released proteins and microbial inactivation would be consistent with this theory. In addition, the comparison of results corresponding to two treatments conditions (25 kV/cm - 20 μs and 18 kV/cm - 400 μs) leading to the same degree of permeabilization (around 90%,) but very different inactivation degrees (10 vs 90%), seem to also support this hypothesis (Fig. 7). Thus, although the exit and/or uptake of the components of lower molecular weight was similar in both treatments, marked differences in protein exit, as measured by the Bradford technique and in the electrophoretic profiles, were observed. From these observations it can also be hypothesized that the transition from reversible to irreversible permeabilization, for *S. aureus* cells treated under our experimental conditions, would be linked to the generation of pores of a size allowing the exit of proteins with a Stokes radius of approx. 1.5 nm. In this way, Saulis and Saulė (2012) already indicated that pores would not be an instantaneous event, but they would be able to grow and stabilize in a short period of time if the electric potential is maintained. They also proposed that shorter treatments applied at higher electric field strength would be able to generate a higher number of pores, but with a lower proportion of large size pores, in comparison to those created in longer treatments applied at a lower electric field strength. Nevertheless, further work should be carried out to verify this hypothesis since other potential explanations for the results obtained cannot be discarded. For instance, it can be hypothesized that the higher proportion of irreversibly permeabilized cells after 18 kV/cm – 400 μs treatments as compared to 25 kV/cm – 20 μs treatments, might also be due to a higher transmembrane transport rate (i.e. faster exit of compounds) or to the generation of damages in other structures such as the cell wall, as described previously (Pillet, Formosa-Dague, Baaziz, Dague, & Rols, 2016). In any case, some evidences seem to discard the first hypothesis, since preliminary work allowed us to verify that these differences in lethality were not due to a difference in the temperature during or after the different treatments (data not shown). Finally, it should also be noted that, at 25 kV/cm, longer treatments led to a decreased proportion of reversibly permeabilized cells too. This strongly suggests that the different proportion of irreversibly permeabilized cells after applying the two treatments compared above (18 kV/cm – 400 μs vs 25 kV/cm – 20 μs) would not be related to the different electric field applied but to the different treatment time. In other words, that increasing treatment time would be the major cause for the shift from reversible to irreversible permeabilization. Furthermore, our results also indicate that, under the conditions here assayed, the exit of proteins of a molecular weight higher than 6 kDa would mainly depend on treatment time, with little influence of the electric field strength. Further work will be required in order to verify these conclusions in a wide range of experimental conditions but, in any case, these results, altogether, also give further support to our hypothesis that pore size determines the reversibility of electroporation of *S. aureus* cells.

On the other hand, pore resealing is also a complex process which is still not completely understood, especially in bacteria. According to the data obtained with model membranes and eukaryotic cells by other researchers, pore resealing process would have different phases, a first one, which is faster and leads to a reduction in pore size and a second

Table 2
Correlation between the log cycles of permeabilizated or inactivated cells with the percentages of released compounds (of the total cellular content for ions and of the total intracytoplasmic soluble content for RNA and proteins) after the different PEF treatments assayed (two electric field strengths and 6 treatment times; see text).

	K^+	Mg^{2+}	RNA	BCA	Bradford	B1	B2
Permeabilization							
Pearson r	0.8946	0.9222	0.9067	0.8513	0.5786	0.5049	0.5212
p value	0.0005	0.0001	0.0003	0.0018	0.0797	0.2019	0.1853
Significative (<0.05)	Yes	Yes	Yes	Yes	No	No	No
Inactivation							
Pearson r	0.5975	0.6351	0.4928	0.6230	0.5699	0.7034	0.7170
p value	0.0681	0.0485	0.1478	0.0544	0.0854	0.0232	0.0196
Significative (<0.05)	No	Yes	No	No	No	Yes	Yes

B1 and B2 correspond to the amount of protein released corresponding to Band 1 and Band 2 of the electrophoresis gels (see text and Fig. 5).

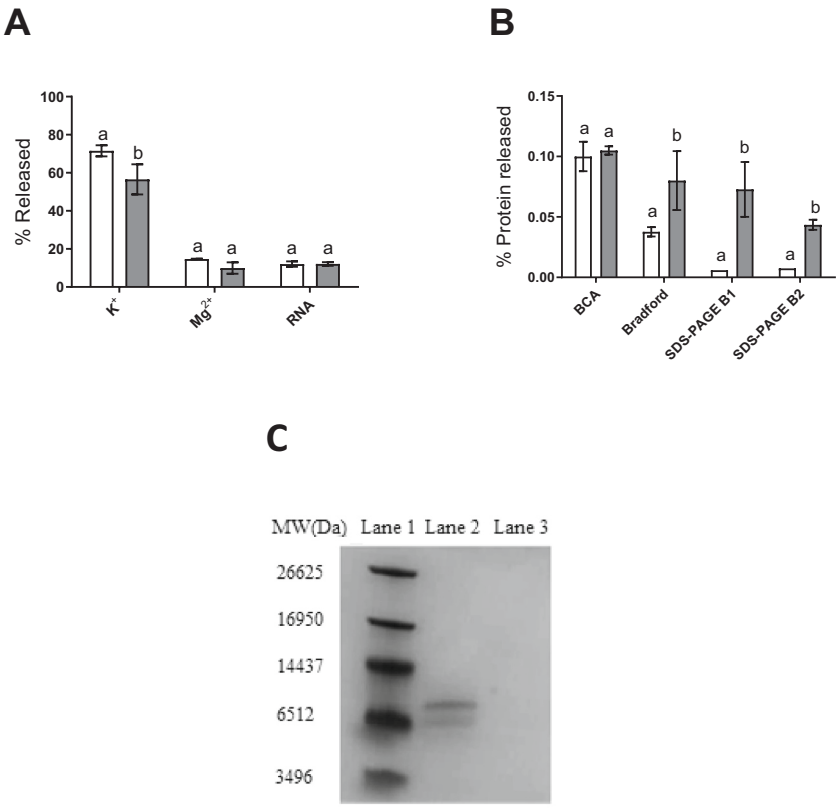

Fig. 7. Component exit (% of the total intracytoplasmic soluble content for ions, RNA and proteins) and electrophoretic profiles of the proteins released after exposing *S. aureus* cells to a PEF treatment of 25 kV/cm for 20 μs (white bars) or of 18 kV/cm for 400 μs (grey bars). A) Ions and RNA exit B) Protein exit measured by BCA, Bradford and through image analysis of SDS-PAGE Tris-Tricine gels. C) Electrophoretic profiles (SDS-PAGE Tris-Tricine gels) of the supernatants of *S. aureus* cells exposed to PEF treatments of 18 kV/cm – 400 μs (Lane 2) or 25 kV/cm – 20 μs (Lane 3). Lane 1: molecular weight marker. Error bars represent the standard deviations. Different letters indicate statistical significant differences ($p < 0.05$) between treatment conditions (student *t*-test).

one, much slower and a biologically active ATP-dependent process, that leads to its complete closure (Pavlin et al., 2008). The process of pore resealing in PEF treated bacteria has only been scarcely studied, but from the existing literature, it can be concluded that in Gram positive bacteria it would also be an ATP-dependent process requiring from minutes to hours to be completed (Somolinos, Espina, Pagán, & Garcia, 2010). However, the mechanisms at the molecular level, involved in pore repair in bacteria are almost unknown and further work is still required in order to elucidate them. In any case, recovery experiments carried out in liquid media showed that whereas cells exposed to 25 kV/cm – 20 μs treatments were able to recover PI impermeability even in the media supplemented with NaCl, as it was already observed and discussed by Cebrián et al. (2015), those treated at 18 kV/cm for 400 μs were not. Therefore, depending on the treatment received, the pore repair ability of *S. aureus* cells was markedly different.

In summary and taken altogether, our data indicate that increasing PEF treatment time would reduce the capability of *S. aureus* cells to repair the electropores formed. Results obtained also suggest that this might be due to the formation of pores of a larger size, which *S. aureus* cells would be unable to reseal in a situation of homeostasis loss (leakage of ions, RNA and proteins). This would explain why the lethality of treatments at 18 kV/cm for 400 μs was higher than that of 25 kV/cm – 20 μs treatments, even the number of electroporated cells was similar after both of them, and why increasing treatment time at 25 kV/cm led to a progressive decrease in the percentage of reversibly electropermeabilized cells. Nevertheless, it cannot be discarded that the exit of a particular protein might be the final cause for the loss of viability in *S. aureus* cells, either because it is a critical component itself or because its loss makes *S. aureus* cells unable to repair the pores/damages caused by PEF. In this sense, two of the proteins identified via LC-ESI-MS/MS (HPr and TrxA) have been proved to be essential or potentially essential to *S. aureus* (Chaudhuri et al., 2009; Postma, Lengeler, & Jacobson, 1993; Prinz, Aslund, Holmgren, & Beckwith, 1997; Uziel, Borovok, Schreiber, Cohen, & Aharonowitz, 2004). HPr is an essential constituyent of the phosphoenolpyruvate-dependent phosphotransferase system, a transport system for carbohydrates in bacteria (Postma et al., 1993). In the second case the thioredoxin system seems to be essential for growth in *S. aureus,* maintaining redox homeostasis, protecting

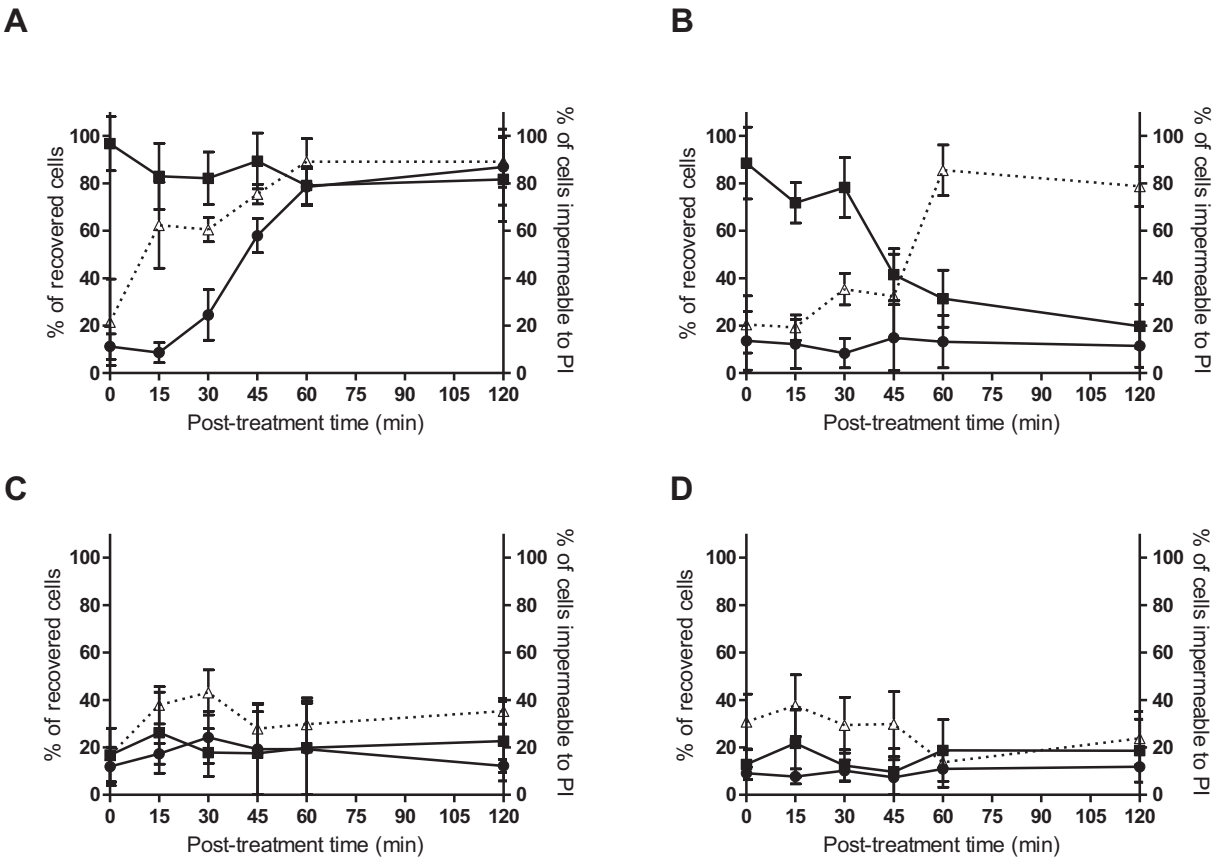

Fig. 8. Influence of recovery time on the percentage of *S. aureus* cells recovered in TSAYE (■) and TSAYE-NaCl (2.39 M) (●) and on the percentage of cells impermeable to PI (Δ) after PEF treatments of 25 kV/cm – 20 μs (A and B) or 18 kV/cm – 400 μs (C and D). Cells were recovered in TSBYE (A and C) or in TSBYE+NaCl (2.39 M) (B and D). Error bars represent the standard deviation.

against reactive oxygen species, and providing electrons to reductive enzymes such as ribonucleotide reductases due to the lack of an alternative glutathione-based system (Uziel et al., 2004). Very relevant cellular functions have also been identified for CopZ, albeit under more specific conditions (Sitthisak, Knutsson, Webb, & Jayaswal, 2007).

The results obtained in this work contribute towards a more precise characterization of *S. aureus* electropermeome. They indicate that release of most compounds, except proteins, was almost immediate after the treatment, but the relative amount released depended on the molecule studied. A good correlation between the release of the smallest components studied (particularly ions) and membrane permeabilization (as measured by NaCl sensitization and PI entry) was observed. On the other hand, results obtained suggest that *S. aureus* inactivation by PEF would be related to the exit of cytoplasmic proteins of a molecular weight higher than 6 kDa. Comparison of two treatments leading to the same level of permeabilization but different levels of inactivation confirmed all the preliminary conclusions and strongly suggests that the increased level of *S. aureus* inactivation attained by treatments at lower electric field strength but of longer duration might be linked to the formation of pores of a higher size. Further work will be required in order to determine to which extent results here obtained can be extrapolated to other prokaryotic cells.

From a practical point of view our results indicate that irreversible permeabilization of *S. aureus* cells would be maximized if long time treatments are applied. However, high electric field – short time treatments might still be more useful/appropriate for food preservation purposes, since treatments would be shorter and with a lower energy input associated. Thus, according to our results, a treatment at 25 kV/cm for 40 μs would attain a similar, or even higher, level of inactivation of *S. aureus* than a 18 kV/cm – 400 μs treatment but would be faster, more energy efficient (81% less energy applied) and would generate an additional log cycle of sublethally damaged cells. On the other hand, our results also suggest that the study of protein leakage might be a very useful tool for further investigating the processes of pore formation and resealing in PEF treated bacteria.

Declaration of interests

The authors declare that they have no known competing financial interests or personal relationships that could have appeared to influence the work reported in this paper.

Acknowledgments

The authors would like to thank Prof. Pawel Mak for kindly supplying the *S. aureus* RN4220 strain expressing GFP through the plasmid pCN6859, Dr. Nabil Halaihel for its help in the image analysis of electrophoresis gels, and the Servicio de Análisis Químico (Servicio General de Apoyo a la Investigación-SAI) of the University of Zaragoza for their technical support in K^+ and Mg^{2+} release measurements. This research received no specific grant from any funding agency in the public, commercial, or not-for-profit sectors.

References

Álvarez, I., Condón, S., & Raso, J. (2006). Microbial inactivation by pulsed electric fields. In J. Raso, & V. Heinz (Eds.), *Pulsed electric field technology for the food industry* (pp. 95–128). Springer Publishing.

Arndt-Jovin, D. J., & Jovin, T. M. (1989). Fluorescence labeling and microscopy of DNA. *Methods in Cell Biology, 30*, 417–448. https://doi.org/10.1016/S0091-679X(08)60989-9

Aronsson, K., Rönner, U., & Borch, E. (2005). Inactivation of *Escherichia coli, Listeria innocua and Saccharomyces cerevisiae* in relation to membrane permeabilization and subsequent leakage of intracellular compounds due to pulsed electric field processing. *International Journal of Food Microbiology, 99*(1), 19–32. https://doi.org/10.1016/j.ijfoodmicro.2004.07.012

Azarashvili, T., Odinokova, I., Krestinina, O., Baburina, Y., Grachev, D., Teplova, V., & Holmuhamedov, E. (2011). Role of phosphorylation of porin (VDAC) in regulation of mitochondrial outer membrane under normal conditions and alcohol intoxication. *Biochemistry (Moscow) Supplement Series A: Membrane and Cell Biology, 5*(1), 11–20. https://doi.org/10.1134/S1990747811010028

Barbosa-Cánovas, G. V., Góngora-Nieto, M. M., Pothakamury, U. R., & Swanson, B. G. (1999). *Preservation of foods with pulsed electric fields*. US: Academic Press.

Batista Napotnik, T., & Miklavčič, D. (2018). In vitro electroporation detection methods – An overview. *Bioelectrochemistry, 120*, 166–182. https://doi.org/10.1016/j.bioelechem.2017.12.005

Bowman, A., Nesin, O., Pakhomova, O., & Pakhomov, A. (2010). Analysis of plasma membrane integrity by fluorescent detection of tl+ uptake. *The Journal of Membrane Biology, 236*(1), 15–26. https://doi.org/10.1007/s00232-010-9269-y

Cebrián, G., Mañas, P., & Condón, S. (2015). Relationship between membrane permeabilization and sensitization of *S. aureus* to sodium chloride upon exposure to pulsed electric fields. *Innovative Food Science and Emerging Technologies, 32*, 91–100. https://doi.org/10.1016/j.ifset.2015.09.017

Chan, Y. G. Y., Frankel, M. B., Missiakas, D., & Schneewind, O. (2016). SagB glucosaminidase is a determinant of *Staphylococcus aureus* glycan chain length, antibiotic susceptibility, and protein secretion. *Journal of Bacteriology, 198*(7), 1123–1136. https://doi.org/10.1128/JB.00983-15

Chaudhuri, R. R., Allen, A. G., Owen, P. J., Shalom, G., Stone, K., Harrison, M., … Charles, I. G. (2009). Comprehensive identification of essential *Staphylococcus aureus* genes using transposon-mediated differential hybridisation (TMDH). *BMC Genomics, 10*(1), 291. https://doi.org/10.1186/1471-2164-10-291

Christian, J. H. B., & Waltho, J. A. (1964). The composition of *Staphylococcus aureus* in relation to the water activity of the growth medium. *Journal of General Microbiology, 35*(2), 205–213. https://doi.org/10.1099/00221287-35-2-205

Chutipongtanate, S., Watcharatanyatip, K., Homvises, T., Jaturongkakul, K., & Thongboonkerd, V. (2012). Systematic comparisons of various spectrophotometric and colorimetric methods to measure concentrations of protein, peptide and amino acid: Detectable limits, linear dynamic ranges, interferences, practicality and unit costs. *Talanta, 98*, 123–129. https://doi.org/10.1016/j.talanta.2012.06.058

Dawson, R. M. C., Elliot, D. C., Elliot, W. H., & Jones, K. M. (1974). *Data for biochemical research* (3rd ed.). Clarendon Press Oxford.

El Zakhem, H., Lanoisellé, J., Lebovka, N. I., Nonus, M., & Vorobiev, E. (2006). The early stages of *Saccharomyces cerevisiae* yeast suspensions damage in moderate pulsed electric fields. *Colloids and Surfaces B: Biointerfaces, 47*(2), 189–197. https://doi.org/10.1016/j.colsurfb.2005.12.010

García, D., Gómez, N., Mañas, P., Raso, J., & Pagán, R. (2007). Pulsed electric fields cause bacterial envelopes permeabilization depending on the treatment intensity, the treatment medium pH and the microorganism investigated. *International Journal of Food Microbiology, 113*(2), 219–227. https://doi.org/10.1016/j.ijfoodmicro.2006.07.007

García, D., Mañas, P., Gómez, N., Raso, J., & Pagán, R. (2006). Biosynthetic requirements for the repair of sublethal membrane damage in *Escherichia coli* cells after pulsed electric fields. *Journal of Applied Microbiology, 100*(3), 428–435. https://doi.org/10.1111/j.1365-2672.2005.02795.x

Gerstberger, S., Hafner, M., & Tuschl, T. (2014). A census of human RNA-binding proteins. *Nature Reviews Genetics, 15*(12), 829–845. https://doi.org/10.1038/nrg3813

Gowrishankar, T. R., Esser, A. T., Vasilkoski, Z., Smith, K. C., & Weaver, J. C. (2006). Microdosimetry for conventional and supra-electroporation in cells with organelles. *Biochemical and Biophysical Research Communications, 341*(4), 1266–1276. https://doi.org/10.1016/j.bbrc.2006.01.094

Graham, J. E., & Wilkinson, B. J. (1992). *Staphylococcus aureus* osmoregulation: Roles for choline, glycine betaine, proline, and taurine. *Journal of Bacteriology, 174*(8), 2711–2716. https://doi.org/10.1128/jb.174.8.2711-2716.1992

Hille, B. (1975). Ionic selectivity of Na and K channels of nerve membranes. *Membranes, 3*, 255.

Hille, B. (2001). *Ionic channels of excitable membranes* (3rd ed.). Sinauer Associates. Inc Publishing.

Ho, S. Y., & Mittal, G. S. (1996). Electroporation of cell membranes: A review. *Critical Reviews in Biotechnology, 16*(4), 349–362. https://doi.org/10.3109/07388559609147426

Kandušer, M., Miklavčič, D., & Pavlin, M. (2009). Mechanisms involved in gene electrotransfer using high- and low-voltage pulses — An in vitro study. *Bioelectrochemistry, 74*(2), 265–271. https://doi.org/10.1016/j.bioelechem.2008.09.002

Kim, S. J., Chang, J., & Singh, M. (2015). Peptidoglycan architecture of gram-positive bacteria by solid-state NMR. *BBA - Biomembranes, 1848*(1), 350–362. https://doi.org/10.1016/j.bbamem.2014.05.031

Kinosita, K., Hibino, M., Itoh, H., Shigemori, M., Hirano, K., Kirino, Y., & Hayakawa, T. (1991). Events of membrane electroporation visualized on a time scale from microsecond to seconds. In D. C. Chang, B. M. Chassy, J. A. Saunders, & A. E. Sowers (Eds.), *Guide to electroporation and electrofusion* (pp. 29–46). Elsevier Inc.

Krassowska, W., & Filev, P. D. (2007). Modeling electroporation in a single cell. *Biophysical Journal, 92*(2), 404–417. https://doi.org/10.1529/biophysj.106.094235

Laborda, F., Medrano, J., & Castillo, J. R. (2004). Influence of the number of calibration points on the quality of results in inductively coupled plasma mass spectrometry. *Journal of Analytical Atomic Spectrometry, 19*(11), 1434–1441. https://doi.org/10.1039/b408512d

Mañas, P., & Pagán, R. (2005). Microbial inactivation by new technologies of food preservation. *Journal of Applied Microbiology, 98*(6), 1387–1399. https://doi.org/10.1111/j.1365-2672.2005.02561.x

Matos, T., Senkbeil, S., Mendonça, A., Queiroz, J. A., Kutter, J. P., & Bulow, L. (2013). Nucleic acid and protein extraction from electropermeabilized *E. coli* cells on a microfluidic chip. *The Analyst, 138*(24), 7347–7353. https://doi.org/10.1039/c3an01576a

Meglic, H. S., Marolt, T., & Miklavcic, D. (2015). Protein extraction by means of electroporation from *E. coli* with preserved viability. *The Journal of Membrane Biology, 248*(5), 893–901. https://doi.org/10.1007/s00232-015-9824-7

Nowakowski, M., Jaremko, Ł., Wladyka, B., Dubin, G., Ejchart, A., & Mak, P. (2018). Spatial attributes of the four-helix bundle group of bacteriocins – The high-resolution structure of BacSp222 in solution. *International Journal of Biological Macromolecules, 107*(Pt B), 2715–2724. https://doi.org/10.1016/j.ijbiomac.2017.10.158

Oshima, T., & Sato, M. (2004). Bacterial sterilization and intracellular protein release by a pulsed electric field. *Advances in Biochemical Engineering/Biotechnology, 90*, 113. https://doi.org/10.1007/b94194

Pavlin, M., Kotnik, T., Miklavčič, D., Kramar, P., & Maček Lebar, A. (2008). Chapter seven electroporation of planar lipid bilayers and membranes. In A. L. Liu (Ed.), *Advances in planar lipid bilayers and liposomes* (pp. 165–226). Elsevier Science & Technology.

Pavlin, M., Leben, V., & Miklavčič, D. (2007). Electroporation in dense cell suspension—Theoretical and experimental analysis of ion diffusion and cell permeabilization. *BBA - General Subjects, 1770*(1), 12–23. https://doi.org/10.1016/j.bbagen.2006.06.014

Pillet, F., Formosa-Dague, C., Baaziz, H., Dague, E., & Rols, M. (2016). Cell wall as a target for bacteria inactivation by pulsed electric fields. *Scientific Reports, 6*(1), 19778. https://doi.org/10.1038/srep19778

Postma, P. W., Lengeler, J. W., & Jacobson, G. R. (1993). Phosphoenolpyruvate: Carbohydrate phosphotransferase systems of bacteria. *Microbiological Reviews, 57*(3), 543–594.

Prinz, W. A., Aslund, F., Holmgren, A., & Beckwith, J. (1997). The role of the thioredoxin and glutaredoxin pathways in reducing protein disulfide bonds in the *Escherichia coli* cytoplasm. *The Journal of Biological Chemistry, 272*(25), 15661. https://doi.org/10.1074/jbc.272.25.15661

Puértolas, E., Luengo, E., Álvarez, I., & Raso, J. (2012). Improving mass transfer to soften tissues by pulsed electric fields: Fundamentals and applications. *Annual Review of Food Science and Technology, 3*(1), 263–282. https://doi.org/10.1146/annurev-food-022811-101208

Raso, J., Alvarez, I., Condón, S., & Sala Trepat, F. J. (2000). Predicting inactivation of *Salmonella Senftenberg* by pulsed electric fields. *Innovative Food Science & Emerging Technologies, 1*(1), 21–29. https://doi.org/10.1016/S1466-8564(99)00005-3

Raso, J., & Barbosa-Cánovas, G. V. (2003). Nonthermal preservation of foods using combined processing techniques. *Critical Reviews in Food Science and Nutrition, 43*(3), 265–285. https://doi.org/10.1080/10408690390826527

Rippe, B., & Stelin, G. (1989). Simulations of peritoneal solute transport during CAPD. Application of two-pore formalism. *Kidney International, 35*(5), 1234–1244. https://doi.org/10.1038/ki.1989.11

Saldaña, G., Puértolas, E., Álvarez, I., Meneses, N., Knorr, D., & Raso, J. (2010). Evaluation of a static treatment chamber to investigate kinetics of microbial inactivation by pulsed electric fields at different temperatures at quasi-isothermal conditions. *Journal of Food Engineering, 100*(2), 349–356. https://doi.org/10.1016/j.jfoodeng.2010.04.021

Saulis, G. (2010). Electroporation of cell membranes: The fundamental effects of pulsed electric fields in food processing. *Food Engineering Reviews, 2*(2), 52–73. https://doi.org/10.1007/s12393-010-9023

Saulis, G., Šatkauskas, S., & Pranevičiūtė, R. (2007). Determination of cell electroporation from the release of intracellular potassium ions. *Analytical Biochemistry, 360*(2), 273–281. https://doi.org/10.1016/j.ab.2006.10.028

Saulis, G., & Saulė, R. (2012). Size of the pores created by an electric pulse: Microsecond vs millisecond pulses. *BBA - Biomembranes, 1818*(12), 3032–3039. https://doi.org/10.1016/j.bbamem.2012.06.018

Sitthisak, S., Knutsson, L., Webb, J. W., & Jayaswal, R. K. (2007). Molecular characterization of the copper transport system in *Staphylococcus aureus*. *Microbiology, 153*(12), 4274–4283. https://doi.org/10.1099/mic.0.2007/009860-0

Somolinos, M., Espina, L., Pagán, R., & Garcia, D. (2010). sigB absence decreased *listeria monocytogenes* EGD-e heat resistance but not its pulsed electric fields resistance. *International Journal of Food Microbiology, 141*(1), 32–38. https://doi.org/10.1016/j.ijfoodmicro.2010.04.023

Sözer, E. B., Levine, Z. A., & Vernier, P. T. (2017). Quantitative limits on small molecule transport via the electropermeome - measuring and modeling single nanosecond perturbations. *Scientific Reports, 7*(1), 57. https://doi.org/10.1038/s41598-017-00092-0

Tarek, M. (2005). Membrane electroporation: A molecular dynamics simulation. *Biophysical Journal, 88*(6), 4045–4053. https://doi.org/10.1529/biophysj.104.050617

Tsong, T. Y. (1991). Electroporation of cell membranes. *Biophysical Journal, 60*(2), 297–306. https://doi.org/10.1016/S0006-3495(91)82054-9

Uziel, O., Borovok, I., Schreiber, R., Cohen, G., & Aharonowitz, Y. (2004). Transcriptional regulation of the *Staphylococcus aureus* thioredoxin and thioredoxin reductase genes in response to oxygen and disulfide stress. *Journal of Bacteriology, 186*(2), 326–334. https://doi.org/10.1128/JB.186.2.326-334.2004

Venturoli, D., & Rippe, B. (2005). Ficoll and dextran vs. globular proteins as probes for testing glomerular permselectivity: Effects of molecular size, shape, charge, and

deformability. *American Journal of Physiology - Renal Physiology, 288*(4), 605–613. https://doi.org/10.1152/ajprenal.00171.2004

Vinothkumar, K. R., & Henderson, R. (2010). Structures of membrane proteins. *Quarterly Reviews of Biophysics, 43*(1), 65–158. https://doi.org/10.1017/S0033583510000041

Weaver, J. C., & Chizmadzhev, Y. A. (1996). Theory of electroporation: A review. *Bioelectrochemistry and Bioenergetics, 41*(2), 135–160. https://doi.org/10.1016/S0302-4598(96)05062-3

Wladyka, B., Piejko, M., Bzowska, M., Pieta, P., Krzysik, M., Mazurek, L., Guevara-Lora, I., Bukowski, M., Sabat, A. J., Frieich, A. W., Bonar, E., Miedzobrodzki, J., Dubin, A., & Mak, P. (2015). A peptide factor secreted by *Staphylococcus pseudintermedius* exhibits properties of both bacteriocins and virulence factors. *Scientific Reports, 5*(1), 14569. https://doi.org/10.1038/srep14569

Zimmermann, U., Pilwat, G., & Riemann, F. (1974). Dielectric breakdown of cell membranes. *Biophysical Journal, 14*(11), 881–899. https://doi.org/10.1016/S0006-3495(74)85956-4